Original article

Textile Research Journal

Textile Research Journal
2014, Vol. 84(12) 1255–1267
© The Author(s) 2014
Reprints and permissions:
sagepub.co.uk/journalsPermissions.nav
DOI: 10.1177/0040517514521118
trj.sagepub.com

SAGE

Electromagnetic shielding properties of woven fabrics made from high-performance fibers

Veronika Šafářová and Jiří Militký

Abstract

The expansion of the electronic industry and the extensive use of electronic equipment in communications, computations, automations, biomedicine, space, and other purposes have led to problems such as electromagnetic interference of electronic devices and health issues. For the reasons given above, the demand for the protection of human beings and sensitive electronic and electrotechnic appliances against the undesirable influence of electromagnetic signals and troublesome charges has been increasing. This paper presents the present state of fabrication and characterization of multifunctional high-performance metal/*m*-aramid hybrid fabrics with increased resistivity to electromagnetic smog while preserving basic properties of textile structures designated for clothing or technical purposes. In this paper, hybrid electromagnetic shielding fabrics made of high-performance fibers are introduced. An effect of metal content is studied and a form of relation between resistivity and total shielding effectiveness is proposed. Furthermore, chosen mechanical properties of developed fabric are evaluated.

Keywords

electromagnetic shielding effectiveness, electrical properties, metal fiber, aramid fiber, hybrid fabrics

According to the World Health Organization,[1] exposure to electromagnetic (EM) fields is not a new phenomenon. However, during the 20th century, environmental exposure to man-made EM fields has been steadily increasing due to growing electricity demand, ever-advancing technologies and changes in social behavior.

Everyone is exposed to a complex mix of weak electric and magnetic fields, both at home and at work. Sources of such emissions could include generation and transmission of electricity, domestic appliances and industrial equipment, telecommunications, and broadcasting. If the EM waves are not isolated effectively, they will cause interference with each other and result in technical errors. If somebody gets exposed under the EM, radiate environment, physical harms may occur to the human body.[2,3]

Metal is considered to be the best EM shielding material due its conductivity and permeability, but it is expensive, heavy, and it may also have thermal expansion and metal oxidation, or corrosion problems associated with its use. In contrast, most synthetic fabrics are electrically insulating and transparent to EM radiation.[4]

In recent years, conductive fabrics have obtained increased attention for EM shielding[5–10] and anti-electrostatic purposes.[11–16] This is mainly due to their desirable flexibility and lightweight properties. One way that conductive fabrics can be created is by using minute electrically conductive fibers. They can be produced in filament or staple lengths and can be incorporated with traditional non-conductive fibers to create yarns that possess varying degrees of conductivity. Another method uses conductive coatings, which can transform substrates into electrically conductive

Faculty of Textile Engineering, Technical University of Liberec, Czech Republic

Corresponding author:
Veronika Šafářová, Faculty of Textile Engineering, Technical University of Liberec, Studentská 2, Liberec 463 17, Czech Republic.
Email: veronika.safarova@tul.cz

materials without significantly altering the existing substrate properties. They can be applied to the surface of fibers, yarns, or fabrics. The most common are metal and conductive polymer coatings.

Meta-aramid is an aromatic polyamide fiber that possesses excellent physical and mechanical properties. Because of its outstanding flame-proof and heat-resisting properties, *m*-aramid fiber can be applied widely in thermal protective apparel. The primary applications in which fabrics are used include firefighting and many industrial areas, such as electrical and molten processing. The EM shielding ability of these protective fabrics is often underestimated. In certain cases, people need to be protected from harmful effects of heat and at the same time they need to be protected from harmful effects of high-level EM radiation (e.g. operators of high-frequency heating or molding apparatus).

There is not enough research on shielding properties of conductive fabrics made of high-performance fibers (designated for protective clothing) produced directly from conductive fibers with increased mechanical properties. Most of the studies focus on composite structures, such as aramid fiber composites.[17–19] For example Zhang et al.[17] prepared cement-based composites by introducing aramid fiber into cement. The effect of the filling ratio and length of fibers on EM and mechanical properties was studied and it was found that both factors had influence on absorption properties, the breaking strength, and the compressive strength of cement. On the other hand, the diameters of the metal fibers utilized in previous studies for EM shielding fabric are too large (0.08–0.15 mm) to be flexible enough to be applied for certain applications.[5,8,12] Therefore, it seems that there is a need for creation of protective fabrics with excellent physical and mechanical properties and at the same time with increased EM shielding ability.

In this study we aimed to design and investigate hybrid high-performance EM shielding fabrics. Woven fabrics are made of hybrid yarns produced by blending extremely thin metal fibers (diameter 0.008 mm) and high-performance *m*-aramid fibers. The design and validation of a low-cost metal composite fabric with EM shielding effectiveness (SE), flexibility, processability, and unique tensile strength is presented. The effect of metal content is studied and a form of relation between resistivity and total SE is proposed. Unique mechanical properties of samples, that have a special ability to shield EM smog, are verified using dynamic mechanic analysis (DMA).

The shielding mechanism

An EM field is built up from electric E and magnetic field H components. An electric field is created by a voltage difference and a magnetic field is created by a moving charge, that is, by a current. Every current is thus accompanied by both an electric and a magnetic field. Electromagnetic interference (EMI) shielding consists of two regions, a near-field shielding region and a far-field shielding region. The amount of attenuation due to shielding depends on the EM wave reflection from the shield surface, absorption of the waves into the shield, and the multiple reflections of the waves at various surfaces or interfaces in the shield. The multiple reflections require the presence of a large surface area (porous or foam) or an interface area (composite material containing fillers with large surface area) in the shields. The loss related with multiple reflections can be neglected when the distance between the reflecting surfaces or interfaces is large compared to the skin depth δ [m] (the penetration depth), defined as:

$$\sigma = \frac{1}{\sqrt{\pi f \mu K}} \tag{1}$$

where f [Hz] is the frequency and μ is the magnetic permeability equal to μ_0. μ_r, μ_0 is the absolute permeability of free space (air $= 4\pi\ 10^{-7}$) and K [S m^{-1}] is the electrical conductivity. An electric field at a high frequency penetrates only the near-surface region of a conductor. The amplitude of the wave decreases exponentially as the wave penetrates the conductor. The depth at which the amplitude is decreased to 1/e of the value at the surface is called the "skin depth," and the phenomenon is known as the "skin effect."[20]

Efficiency of EM shields is commonly expressed by the total SE [dB], which represents the ratio between power P_2 [W] obtained when the shield is present and power P_1 obtained when the shield is not present:[18]

$$SE = -10\log\left(\frac{P_2}{P_1}\right) \tag{2}$$

where $\log(x)$ is decimal logarithm.

The EM shielding efficiency of an element is characterized by its electric conductivity, permittivity, and permeability, parameters of source, and properties of the ambient surrounding.

Whilst we are able to determine SE for metal shields on the basis of their electrical parameters, for samples with a more complex structure, and often heterogeneous composition, such as textile materials, it seems that the SE can be determined only based on measurement.[21] There are several methods available for SE measurements. However, for thin planar structures, there are no standards defining the evaluation of small samples of only several tens of centimeters in size. The following test methods are commonly used

for measuring EM shielding of a given shielding material:[22]

1. the shielded box method;
2. the shielded room method;
3. the coaxial transmission line method.

Each of the above-mentioned methods has some advantages and limitations. For example, the shielded box method is widely used for fast, comparative measurements of test samples of different materials. The test comprises of a metal box that has a sample port in one wall and is fitted with receiving antenna. A transmitting antenna is placed outside the box.[22] Great shielding of surrounding man-made noise is the main advantage of this measurement method. On the other hand, for particularly narrow frequency ranges, a metal box with specific dimensions is required. The coaxial transmission line method (ASTM D4935) is now the most commonly preferred method. The measurements can be done at a specific frequency range (from 30 MHz to 1.5 GHz). The results obtained in different laboratories should be comparable.[21] Tests are carried out on small doughnut-shaped samples, but preparation of the samples is quite time consuming. MIL-STD-285, IEEE-STD-299, and later standards (e.g. EN 61000-5-7) based on the shielded room method are marked as the most sophisticated ones.[22] The test specimen size ranges typically from 0.25 to 2.5 m^2 in area for square samples or round test samples with a diameter of 30 cm.[21] In general, a signal source is placed outside the test enclosure, whilst the measurement device is located inside. The frequency range is from about 100 kHz to 10 GHz.[5] It is expected that the test results obtained for the same material tested at different laboratories can vary, even by as much as several dBs.[21] This is because the opening in the shielded wall of the chamber also affects the measurements. This opening itself forms a type of antenna with the parameters depending on several factors, one of which is its dimensions.

As already mentioned above, the evaluation of EM interference shielding efficiency needs to use special devices. Besides that, there is no measurement method that would singularly define the SE parameters of screening textiles and also no effective method for comparing the results of SE measurement obtained via different test methods based on different physical principles (for example MIL-STD 285 and ASTM D4935).[21] Measurements of volume resistivity or reciprocal values of electric conductivity are simpler. It is known from the theory that at sufficiently high frequencies it is possible to measure characteristics of the electrical part of the EM field only and therefore there should be a direct relation between total SE [dB] and fabric resistivity. Basic proposed numerical models of fabric SE are based either on electrical properties (especially volume conductivity) of the element[23–28] or on analysis of leakage through the opening in the textile.[29]

Experimental details

Hybrid yarns

Hybrid yarns were composed of high-performance meta-aramid fibers and different content of staple BEKINOX stainless steel (SS) metal fibers (1%, 3%, 5%, 10%, 15%, 20%). The aspect ratio (length/diameter ratio, l/d) of the SS used in this study is 6250, since the diameter of the SS is 8 μm and the fiber length of the SS is 50 mm. In this study, CONEX high-performance poly(*m*-phenylene isophthalamide) fiber with a fineness 1.8 dtex and 51 mm length was used. TREVON polypropylene fiber (2.2 dtex/50 mm) was chosen as a comparative non-conductive material. Properties of these fibers are given in Table 1. Hybrid yarns were two-ply yarns; fineness of yarns was 2×25 tex.

Hybrid fabrics

The seven fabrics with the same structure (weft and warp fineness 2×25 tex, warp density 20 1/cm, weft density 19 1/cm and twill weave) were used. Details about the fabrics are given in Table 2. Sample No. 7 was used in order to compare whether the average difference between the chosen mechanical properties of samples with different non-conductive portions is significant.

Table 1. Properties of fibers used for this study

Fiber	Fineness [tex]	Length [mm]	Tensile strength [cN/tex]	Elongation [%]	Young's modulus [cN/dtex]
Meta-aramid fiber (Conex)	1.80	51	34.38	32.2	57.37
Stainless steel fiber (Bekinox)	3.85	50	14.35	1.29	111.56
Polypropylene fiber (Trevon)	2.20	50	34.83	57.57	24.95

Table 2. Characteristics of fabrics

Sample	Composition	Warp/weft count [tex]	Fabric thickness [mm]	Fabric structure	Warp/weft density [1/cm]	Mass per unit area [g/m^2]
1	1% SS/99% *m*-aramid	25 × 2/25 × 2	0.70	2/2 twill	20/19	211
2	3% SS/97% *m*-aramid	25 × 2/25 × 2	0.63	2/2 twill	20/19	215
3	5% SS/95% *m*-aramid	25 × 2/25 × 2	0.57	2/2 twill	20/19	213
4	10% SS/80% *m*-aramid	25 × 2/25 × 2	0.58	2/2 twill	20/19	208
5	15% SS/75% *m*-aramid	25 × 2/25 × 2	0.58	2/2 twill	20/19	212
6	20% SS/80% *m*-aramid	25 × 2/25 × 2	0.57	2/2 twill	20/19	215
7	5% SS/95% PP	25 × 2/25 × 2	0.77	2/2 twill	20/19	230

SS: stainless steel; PP: polypropylene.

Statistical analysis of small samples

Due to the very small sample sizes $4 \le n \le 20$ available for evaluation process, a procedure based on order statistics introduced by Horn[30] was used. This is based on the depths that correspond to the sample quartiles. The pivot depth is expressed by:

$$H_L = \text{int}[(n+l)/2]/2 \text{ or } H_L = \text{int}[(n+l)/2+l]/2$$

according to which H_L is an integer. The lower pivot is $x_L = x_{(H)}$ and the upper one is $x_U = x_{(n+1-H)}$. Note that the $x_{(i)}$ are ordered statistics, that is, $x_{(i)} <= x_{(i+1)}$. The estimate of the parameter of location is then expressed by the *pivot half sum*:

$$P_L = 0.5(x_L + x_U) \tag{3}$$

and the estimate of the parameter of spread is expressed by the *pivot range*:

$$R_L = (x_U - x_L). \tag{4}$$

The random variable

$$T_L = \frac{P_L}{R_L} = \frac{x_L + x_U}{2(x_U - x_L)} \tag{5}$$

has approximately symmetric distribution and its quantiles are given by Horn.[30]

The 95% confidence interval of the mean is expressed by pivot statistics as

$$P_L - R_L t_{L,0.95}(n) \le \mu \le P_L + R_L t_{L,0,95}(n) \tag{6}$$

and analogously hypothesis testing may also be carried out. For small samples ($4 \le n \le 20$), the pivot statistics lead to more reliable results than the application of Student's *F*-test or robust *t*-tests.

Characterization

Electrical properties evaluation. Volume and surface resistivity of the high-performance hybrid fabrics were measured according to the standard ASTM D257-07, at temperature $T = 22.3^{\circ}$C and relative humidity $RH = 40.7\%$. Volume resistivity is measured by applying a voltage potential across opposite sides of the sample and measuring the resultant current through the sample. Volume resistivity ρ_V [Ω . cm] was calculated from the following relation:

$$\rho_V = R_V \frac{S}{t} \tag{7}$$

where R_V [Ω] is volume resistance reading, t is thickness of the fabric [cm], and S is the surface area of the electrodes [cm^2].

Surface resistivity is measured by applying a voltage potential between two electrodes of specified configuration that are in contact with the same side of a material under test. Surface resistivity ρ_S [Ω] was calculated from relation:

$$\rho_S = R_S \frac{2\pi}{\ln\left(\frac{R_2}{R_1}\right)} \tag{8}$$

where R_S [Ω] is the surface resistance reading, R_1 is the outer radius of the center electrode [m], and R_2 is the inner radius of the outer ring electrode [m]. The measurement was carried out at 15 different places on the textile samples because of subsequent statistical analysis, $\alpha = 0.05$, $t_{L,0.95}(15) = 0.399$. The mean values estimator (pivot half sums), pivot ranges, and confidence intervals for means of ρ_V and ρ_S are summarized in Table 3.

Electromagnetic shielding effectiveness evaluation. The SE of the high-performance hybrid fabrics was measured according to ASTM D 4935-99,[29] for planar materials

Table 3. Results of electrical properties' evaluation

	Volume resistivity ρ_V [Ω.cm]			Surface resistivity ρ_s [Ω]		
Sample	Pivot half sum P_L	Pivot range R_L	95% CI	Pivot half sum P_L	Pivot range R_L	95% CI
1	4.16E + 08	3.10E + 08	± 1.24E + 08	3.24E + 07	2.68E + 07	± 1.07E + 07
2	6.48E + 06	4.88E + 06	± 1.95E + 06	1.14E + 06	9.83E + 05	± 3.92E + 05
3	1.32E + 06	1.07E + 06	± 4.26E + 05	3.11E + 05	2.43E + 05	± 9.71E + 04
4	6.49E + 04	3.51E + 04	± 1.40E + 04	3.43E + 04	1.81E + 04	± 7.21E + 03
5	1.04E + 04	4.97E + 03	± 1.98E + 03	3.47E + 03	1.44E + 03	± 5.76E + 02
6	6.14E + 03	1.63E + 03	± 6.51E + 02	1.19E + 03	6.28E + 02	± 2.51E + 02

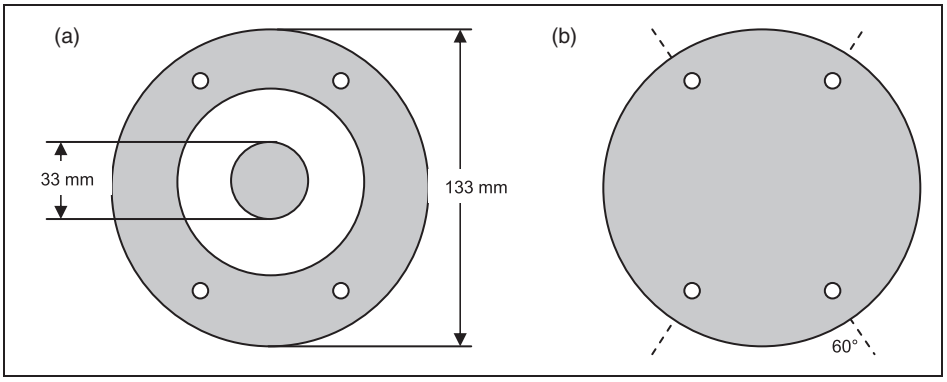

Figure 1. Illustrations of (a) reference and (b) load sample.

using a plane-wave, far-field EM wave. The SE of samples was measured over a frequency range from 30 MHz to 1.5 GHz. The set-up consisted of a sample holder with its input and output connected to the network analyzer. A SE test fixture (Electro-Metrics, Inc., model EM-2107A) was used to hold the sample. The design and dimension of the sample holder follows the ASTM method mentioned above. Network analyzer Agilent E5061B was used to generate and receive the EM signals. The standard mentioned above determines the SE of the fabric using the insertion-loss method. A reference measurement for the empty cell was required for the SE assessment. A "through" calibration with the help of the reference sample was made first. A load measurement was performed on a solid disk-shape sample subsequently. The reference and load specimens must be of the same material and thickness. Sample (both reference and load) geometries according to ASTM D 4935-99 are shown in Figure 1. The measurement was carried out at four different places on the textile samples because of subsequent statistical analysis, $\alpha = 0.05$, $t_{L,0.95}(4) = 0.555$. The mean values estimator (pivot half sums), pivot ranges, and confidence intervals for means of SE for frequency 1.5 GHz are summarized in Table 4.

Chosen mechanical properties' evaluation. Young's modulus E and loss factor $tg\ \delta$ were chosen as representative candidates for mechanical properties' evaluation. These parameters were studied with the help of the DMA method. The DMA method monitors the behavior of materials during mechanical exposure. The viscoelastic property of a sample is studied using DMA where a sinusoidal force (stress σ) is applied to a material and the resulting displacement (strain ε) is measured. This sinusoidal force was chosen as the easiest way to simulate dynamic conditions during wearing, because developed high-performance fabrics are designed for protective clothing. For a perfectly elastic solid, the resulting strain and stress will be perfectly in phase. Viscoelastic polymers have the characteristics in between where the same phase lag will occur during DMA tests. This phase lag represents loss angle δ (see Figure 2). Loss factor $tg\ \delta$ expresses the rate of mechanical loss; it is a portion between loss and storage modulus:

$$\tan\delta = \frac{E''}{E'} = \frac{E\sin\delta}{E\cos\delta} \tag{9}$$

where E is a complex modulus, E'' is a loss modulus, and E' is a storage modulus.

Table 4. Results of electromagnetic shielding effectiveness evaluation

	Electromagnetic shielding effectiveness *SE* [dB] $f = 1.5$ GHz		
Sample	Pivot half sum P_L	Pivot range R_L	95% CI
1	12.97	1.47	±0.59
2	22.36	0.92	±0.37
3	25.9	2.88	±1.15
4	29.58	2.15	±0.86
5	33.51	1.05	±0.42
6	35.98	0.65	±0.26

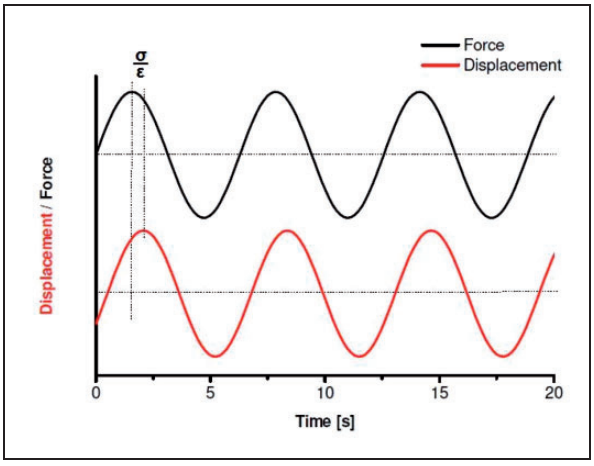

Figure 2. Phase diagram: time behavior of force and diplacement.

Firstly, the conductive component content on the Young's modulus and loss factor was studied. For this purpose, samples containing different portions of SS fiber and identical non-conductive components were used (sample no. 1–6). Although there are many studies comparing the mechanical performances of fibers/fabrics made of *m*-aramid and polypropylene, it was aimed to find out if the non-conductive component itself has a statistically significant effect on the Young's modulus of these hybrid samples designed for protective clothing. Therefore, in the second step, the effect of the non-conductive component on mechanical properties was examined. On this occasion samples with the same content of conductive component (5%) and different material using a similar non-conductive component (*m*-aramid, polypropylene) were evaluated (sample no. 3, sample no. 7). All studied samples have the same structure (weft and warp fineness 2×25 tex, warp sett 20 1/cm, weft sett 19 1/cm, and twill weave). The measurement was carried out at four different places on the textile samples because of subsequent statistical analysis, $\alpha = 0.05$, $t_{L,0.95}(4) = 0.555$. The mean values (pivot half sums), pivot ranges, confidence intervals for means of the Young's modulus, and loss factor are summarized in Tables 5 and 6.

Results and discussion

As described above, textile samples made of yarns containing meta-aramid fibers and different portions of conductive metal fiber (sample no. 1–6) were characterized by their electrical properties (surface and volume resistivity), EM shielding (coaxial transmission line method), and chosen mechanical properties (Young's modulus). Samples with different material using a similar non-conductive component (sample no. 3, sample no. 7) were also evaluated in the terms of the Young's modulus.

In order to get a clear overview of the results, Table 7 summarizes mean values of resistivity, EM SE, and the Young's modulus of samples with different material composition. All statistical parameters of the measured data (mean values, spread, and confidence intervals) are represented in Tables 3–6. Table 7 shows that volume and surface resistivity are decreasing (by about five orders) with increasing content of metal fiber inside the woven fabric. EM SE is increasing (up to 36 dB for samples with 20% of conductive component at frequency 1.5 GHz) with increasing conductivity of samples, which falls in line with the shielding theory. We can observe that the Young's modulus is increasing with increasing metal fiber content in samples for both studied directions.

Electrical properties

Figure 3 depicts the volume resistivity ρ_V and surface resistivity ρ_s metal fiber concentration curve for current samples made of high-performance fibers (sample no. 1–6). A strong correlation was found; the volume and surface resistivity decrease by more than four orders of magnitude between 1% and 20% metal fibers in the hybrid fabrics. This figure also identifies a percolation threshold at a loading of 3% of conductive component. A percolation threshold and drastic decrease in resistivity exists where the volume fraction of the metal fiber portion becomes sufficient to provide continuous electrical paths through the non-conductive component. Generally, the percolation threshold varies considerably with the shape and agglomeration of the conductive phase, as well as the type of non-conductive phase used. It is well known that the resistivity dependence on the amount of conductive component P is different for the range below and above the so-called percolation threshold P_o. The ρ_V and ρ_s show the strongly

Table 5. Details of studied fabric for Young's modulus evaluation

	Young's modulus [GPa]					
	Warp direction			Weft direction		
Sample	Pivot half sum P_L	Pivot range R_L	95% CI	Pivot half sum P_L	Pivot range R_L	95% CI
1	8.95E-02	1.52E-02	±8.44E-03	8.74E-02	1.18E-02	±6.55E-03
2	9.43E-02	1.55E-02	±8.60E-03	1.07E-01	1.63E-02	±9.05E-03
3	9.13E-02	4.70E-03	±2.61E-03	1.07E-01	1.00E-02	±5.55E-03
4	1.03E-01	4.00E-03	±2.22E-03	1.28E-01	1.50E-02	±8.33E-03
5	1.06E-01	8.00E-03	±4.44E-03	1.34E-01	1.33E-02	±7.38E-03
6	1.18E-01	6.00E-03	±3.33E-03	1.44E-01	1.20E-02	±6.66E-03
7	5.96E-02	1.20E-03	±6.66E-04	7.37E-02	7.40E-03	±4.11E-03

Table 6. Details of studied fabric for loss factor evaluation

	Loss factor [-]					
	Warp direction			Weft direction		
Sample	Pivot half sum P_L	Pivot range R_L	95% CI	Pivot half sum P_L	Pivot range R_L	95% CI
1	2.45E-01	3.90E-02	±2.16E-02	2.48E-01	1.60E-02	±8.88E-03
2	2.38E-01	2.30E-02	±1.28E-02	2.54E-01	3.20E-02	±1.78E-02
3	2.59E-01	2.90E-02	±1.61E-02	2.31E-01	1.00E-02	±5.55E-03
4	2.36E-01	1.80E-02	±9.99E-03	2.34E-01	5.10E-02	±2.83E-02
5	2.62E-01	4.20E-02	±2.33E-02	2.24E-01	2.80E-02	±1.55E-02
6	2.64E-01	1.60E-02	±8.88E-03	2.33E-01	5.10E-02	±2.83E-02
7	2.84E-01	6.00E-03	±3.33E-03	2.61E-01	5.00E-03	±2.78E-03

Table 7. Mean values of samples' studied characteristics

Sample	Composition	Volume resistivity ρ_V [Ω.cm]	Surface resistivity ρ_s [Ω]	Electromagnetic shielding effectiveness *SE* [dB], $f = 1.5$ GHz	Young's modulus [GPa]	
					Warp direction	Weft direction
1	1% SS/99% *m*-aramid	4.16E + 08	3.24E + 07	12.97	8.95E-02	8.74E-02
2	3% SS/97% *m*-aramid	6.48E + 06	1.14E + 06	22.36	9.43E-02	1.07E-01
3	5% SS/95% *m*-aramid	1.32E + 06	3.11E + 05	25.9	9.13E-02	1.07E-01
4	10% SS/80% *m*-aramid	6.49E + 04	3.43E + 04	29.58	1.03E-01	1.28E-01
5	15% SS/75% *m*-aramid	1.04E + 04	3.47E + 03	33.51	1.06E-01	1.34E-01
6	20% SS/80% *m*-aramid	6.14E + 03	1.19E + 03	35.98	1.18E-01	1.44E-01
7	5% SS/95% PP	–	–	–	5.96E-02	7.37E-02

SS: stainless steel; PP: polypropylene.

decreasing function of P below P_o . The ρ_V and ρ_s show the more slowly decreasing function of P in the range above P_o for samples 1–6 . It stands to reason that resistivity will not increase dramatically with additional increasing of the conductive component (above 20%).

The dependence of resistivity (ρ_V, ρ_s) on P can be expressed by a simple power function (see Figure 4; adopted from Clingerman et al.[31]):

$$\rho = \rho_C \cdot P^E \tag{10}$$

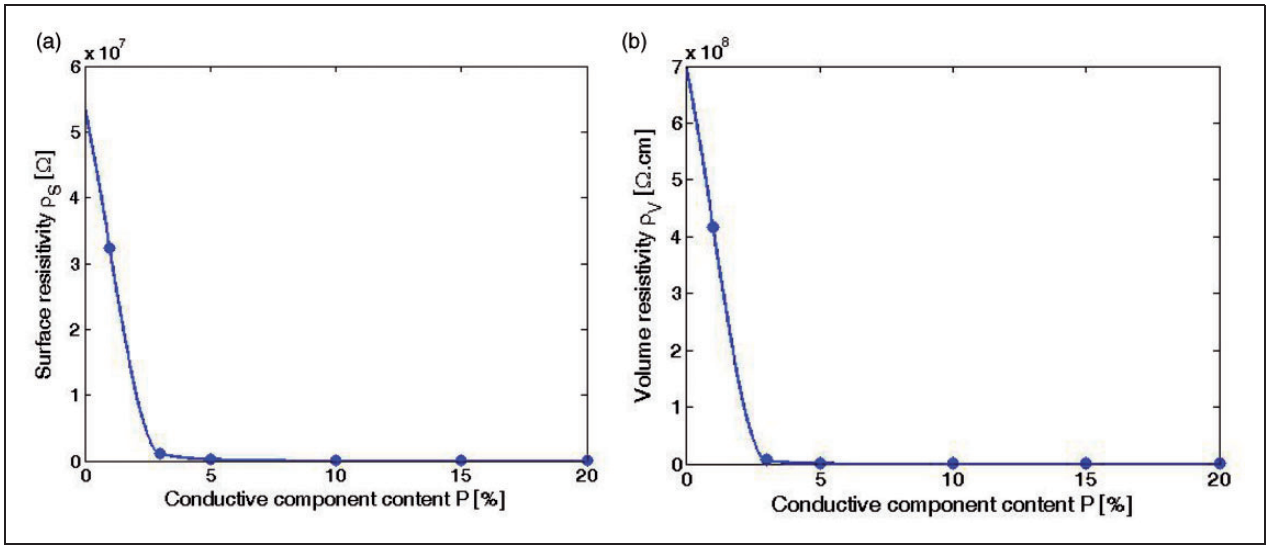

Figure 3. The dependence of (a) surface resistivity and (b) volume resistivity of samples on percentage of conductive component.

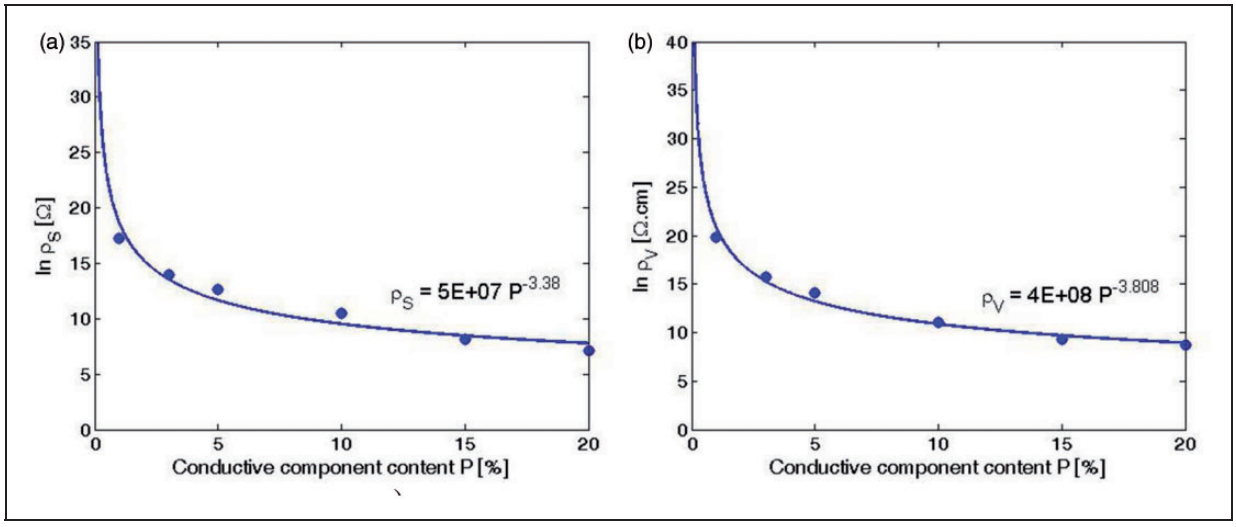

Figure 4. The dependence of the natural logarithm of (a) surface resistivity and (b) volume resistivity of samples on percentage of conductive component approximated by the simple power function.

where ρ is the volume or surface resistivity, ρ_C is the surface or volume resistivity for $P = 1\%$ of the conductive component in hybrid yarn, and parameter E is dependent on the structure of the conductive component.

Electromagnetic shielding efficiency

Figure 5 shows the variation in SE for the six fabrics made of high-performance fibers with incident frequency in the range 30–1500 MHz. The fabric with the highest content of conductive component (metal fiber) has the highest shielding efficiency through the frequency range. The effect of metal content on the SE has been already well established (e.g. Cheng et al.,[4] Duran and Kadoglu,[8] and Kim et al.[32]). It was confirmed in this study that SE increases with increasing metal fiber content. The position of the SE global maximum is possible to observe about frequency 1.1 GHz for all samples. The sample with the highest content of metal fiber reaches 42.9 dB for this frequency. It is possible to observe a shift of the local minimum/maximum to lower frequencies for samples with higher metal content.

The dependence of SE for frequency 1.5 GHz on metal fiber content in yarn is shown in Figure 6(a). We can examine the percolation threshold of the

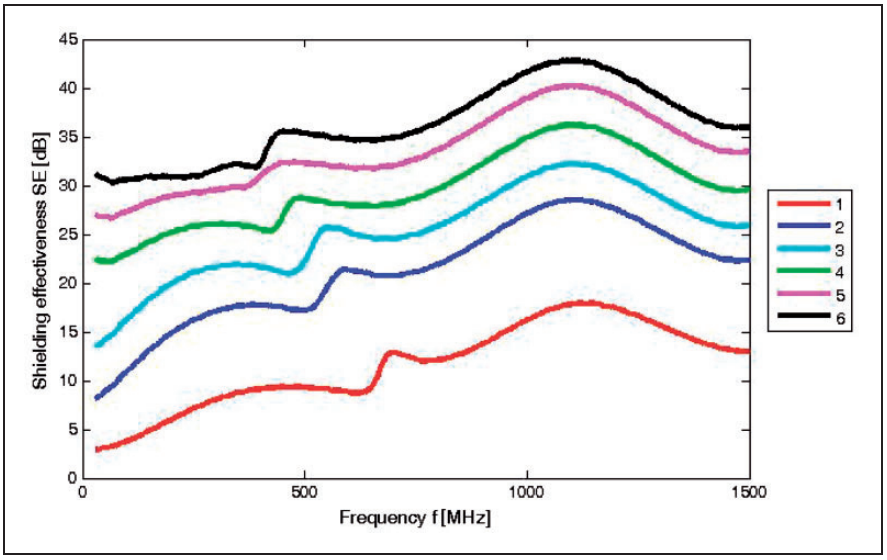

Figure 5. The dependence of shielding effectiveness on frequency for all samples.

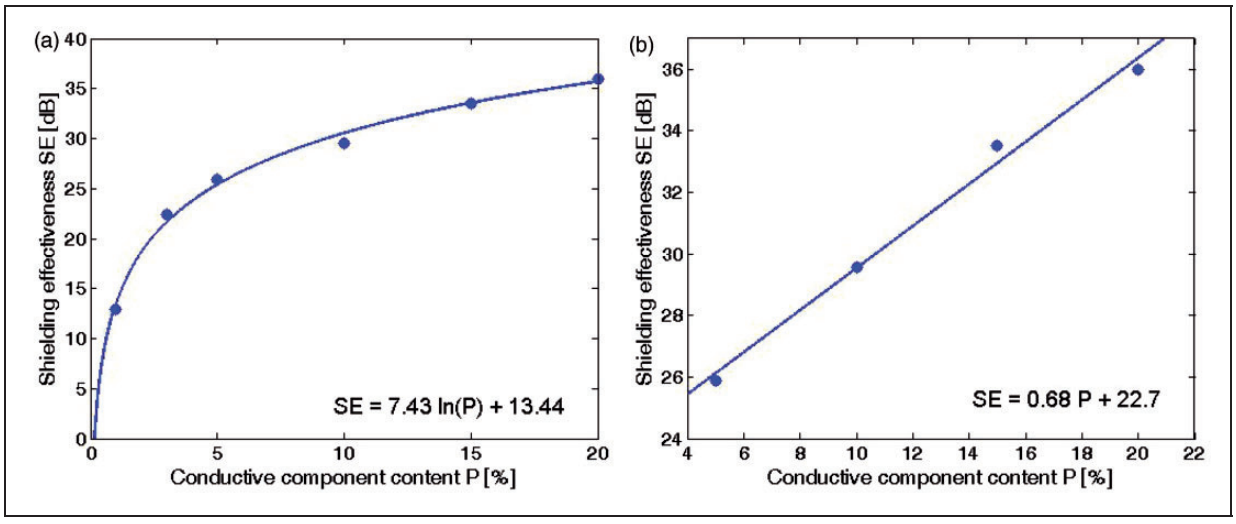

Figure 6. The dependence of shielding effectiveness on conductive component content for (a) the whole range of samples and (b) samples above the percolation threshold.

conductive component, which is about 3%. Even though the SE of samples was obviously frequency dependent, the SE increased logarithmically with metal content. The dependence of SE on P for the range above P_0 can be simply approximated by lines (see Figure 6(b)). The solid line in this graph corresponds to the linear regression model with parameters obtained by the minimizing sum of squared differences. This linear regression model can be used for prediction of the value of P for sufficient shielding. For example, for samples no. 1–6:

$$P = \frac{SE - 22.7}{0,68} \tag{11}$$

For example, $SE = 40\,\text{dB}$ can be obtained at conductive component concentration $P = 25.44\%$. The prediction ability of this line model is restricted to the content of the conductive component above percolation threshold P_o.

Correlation between electric resistance and electromagnetic shielding

It is well known that the SE increases as electric conductivity as well as permittivity of shielding material increases based on the EM shielding theory,[32,33] but there is a lack of experimental verification and

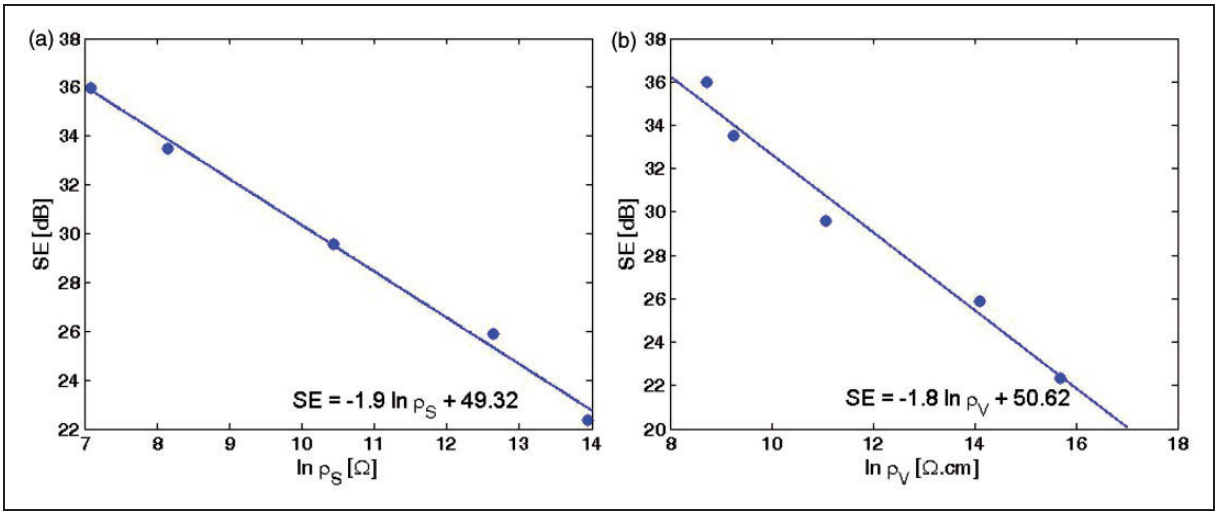

Figure 7. The dependence of shielding effectiveness on the logarithm of (a) the surface and (b) volume resistivity in the area above the percolation threshold.

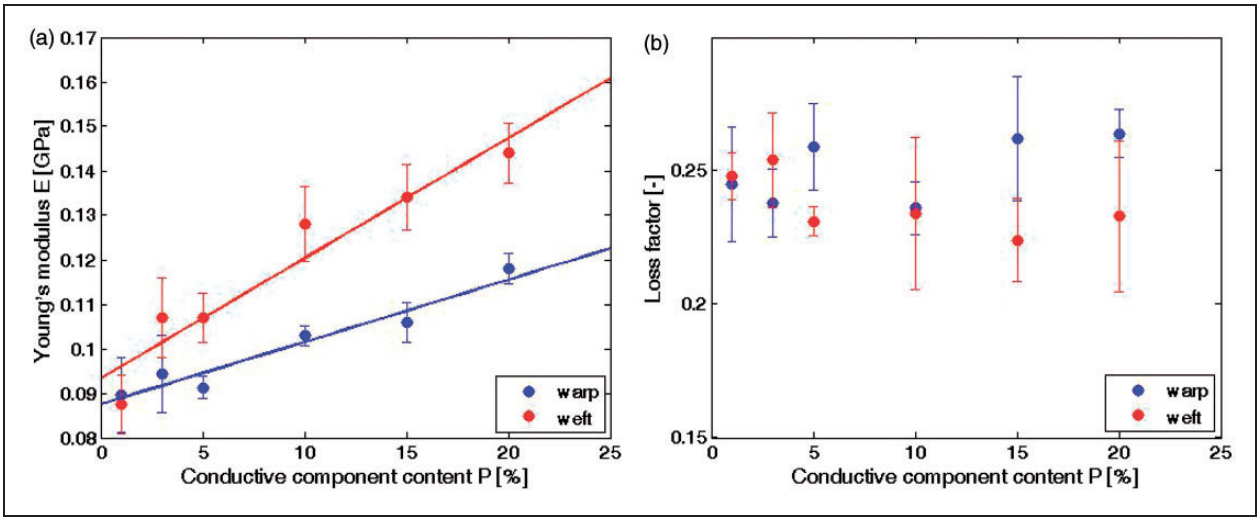

Figure 8. The dependence of (a) the Young's modulus and (b) the loss factor on conductive component content.

exploration of this dependence for fiber structures. In addition, direct measurement of fabrics' EM SE is quite complicated, especially because of the need for special devices and time-consuming preparation of samples. Utilization of the presumption that the electrical part of the EM field dominates for sufficiently high frequencies seems to be simpler. Knowledge of the electrical characteristics, which are easily measurable, could be therefore used for establishment of EM SE of textile samples. That is why correlation between surface and volume resistances and EM shielding efficiency is studied. Samples with content of conductive component higher than $P = 3\%$ were analyzed because they belong to the region above the percolation threshold. The dependence of total SE on logarithms of surface and volume resistivity log ρ_s and log ρ_V is shown in Figure 7. The approximate linearity is visible. The solid lines in this graph correspond to the linear regression model with parameters obtained by the minimizing sum of squared differences. The corresponding correlation coefficient $r = 0.997$, resp. 0.9878 indicates the good quality of fit. This graph clearly indicates that for sufficiently high frequencies it is sufficient to measure only the electric field characteristics. In this graphical evaluation, EM shielding efficiency at only one frequency (1.5 GHz) was studied. This particular frequency is the maximum one for measuring SE by the coaxial transmission line method. During the research it was confirmed that linear regression model is applicable also for other

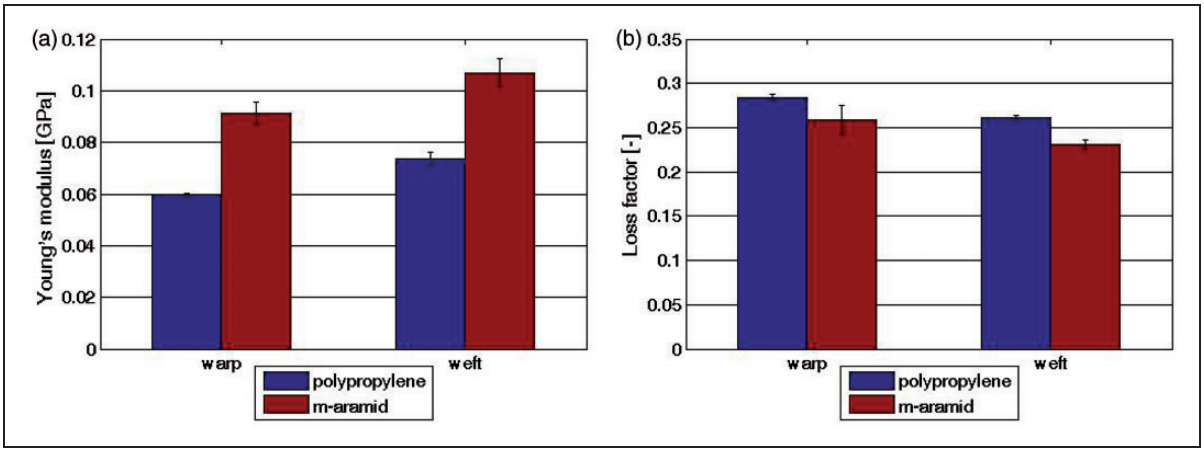

Figure 9. The dependence of (a) the Young's modulus and (b) the loss factor on different types of non-conductive components of samples.

Table 8. Specified requirements of electromagnetic shielding textiles.[34]

Grade	5 Excellent	4 Very good	3 Good	2 Moderate	1 Fair
Percentage of electromagnetic shielding (ES)	SE > 99.9%	99.9% ≥ SE > 99%	99% ≥ SE > 90%	90% ≥ SE > 80%	80% ≥ SE > 70%
Shielding effectiveness (SE)	SE > 30 dB	30 dB ≥ SE > 20 dB	20 dB ≥ SE > 10 dB	10 dB ≥ SE > 7 dB	7 dB ≥ SE > 5 dB

studied frequencies (900 MHz–1.5 GHz) with good quality of fit ($r = 0.99$–0.98).

Chosen mechanical properties

The effect of content of conductive fiber content on Young's modulus is shown in Figure 8(a). The solid line in this graph corresponds to the linear regression model with parameters obtained by the minimizing sum of squared differences. It is clear that the Young's modulus increases with the increasing portion of metal fiber in the sample. The Young's modulus of weft is higher in comparison with the Young's modulus of warp. The same effect on the loss factor is shown in Figure 8(b). There is no clear dependence between the loss factor and conductive component content.

The effect of non-conductive material (*m*-aramid versus polypropylene) on the Young's modulus is shown in Figure 9(a). The same effect on the loss factor is shown in Figure 9(b). As expected, we can observe that the Young's modulus is much higher when *m*-aramid fiber is used. The difference is about 30 MPa for the weft and warp directions. Samples made of *m*-aramid fiber have a lower loss factor in comparison with samples made of polypropylene, which is in agreement with the Young's modulus evaluation. This effect is determined by properties of fibers used in this study (see Table 1). It was confirmed that content of SS fiber (1–20%), as well as the type of non-conductive component (*m*-aramid versus polypropylene fiber), has a statistically significant effect on the Young's modulus.

Conclusion

The EM shielding properties and Young's modulus of conductive woven fabrics made of metal and high-performance fibers were investigated assuming to use these fabrics in protective clothing. As high-performance fibers, meta-aramid fibers were considered. A linear relationship between the conductive component concentration (above the percolation threshold) and SE of the fabrics was also derived.

Weft fabrics with the same structure and different portion of conductive phase in hybrid yarn were studied. Hybrid yarns forming weaves were composed of *m*-aramid and staple SS fiber. Samples were characterized by their volume and surface resistivity (standardized method). Plane-wave shielding properties of the composite high-performance fabric were measured between 30 and 1500 MHz using the coaxial transmission line method.

The so-called percolation threshold, dependence of resistivity, and total SE on the amount of conductive

component in hybrid yarn and dependence of total SE on volume resistivity and surface resistivity was examined. It is clear that the portion of the conductive component has a significant effect on increasing conductivity (decreasing resistivity) and improvement of EM shielding efficiency. Samples with the highest content of conductive component have EM shielding efficiency higher than 35 dB for frequency 1.5 GHz, which means that more than 99.9% (see Table 8) of EM waves were shielded by the high-performance conductive fabrics. It is possible to express dependence between resistivity and percentage of the conductive phase in hybrid yarn by a simple power function adopted from the literature. It is possible to express the dependence between total SE and percentage of conductive phase in hybrid yarn above the percolation threshold P_0 using the linear regression model. A model for prediction of the value P for desired shielding was proposed. It was shown that dependence of total SE on volume and surface resistivity of fabric above percolation threshold V_0 is nearly linear at the frequency of 1.5 GHz. For reasons given above, the existence of the direct relation between electrical properties and the ability of the sample to shield a plane-wave EM field was confirmed.

It was found out that increasing the conductive component content has an effect on increasing the Young's modulus, while *m*-aramid as a non-conductive component of a sample significantly influences the chosen mechanical properties (Young's modulus) of samples. Therefore, so-called high performance was proved.

It was also ascertained that these high-strength fabrics with optimum EM SE can be obtained by controlling the content of the conductive component. Samples prepared in this study have not only a very satisfactory SE level (see Table 8), but they also have very good mechanical properties appropriate for the chosen application (e.g. protective clothing).

Funding

This work was supported by the research project TIP–MPO VaV 2009 ''Electromagnetic field protective textiles with improved comfort'' of the Czech Ministry of Industry.

References

1. World Health Organization. *Establishing a dialogue on risks from electromagnetic fields*. Geneva: WHO, 2002.
2. Bolte JFB and Pruppers MJM. *Electromagnetic fields in the working environment*. Netherlands: Ministry of Social Affairs and Employment (SZW) report, 2006.
3. Polisky LE. *Radiation hazards issues for telecommunication facility professionals*. Ashburn, VA: Comsearch, 2005.
4. Cheng KB, Cheng TW, Lee TC, et al. Effects of yarn constitutions and fabrics specifications on electrical properties of hybrid woven fabrics. *Composites Part A* 2003; 34: 971–978.
5. Ortlek HG, Alpyildiz T and Kilic G. Determination of electromagnetic shielding performance of hybrid yarn knitted fabrics with anechoic chamber. *Textil Res J* 2013; 83: 90–99.
6. Chen H, Lee KC, Lin JH, et al. Fabrication of conductive woven fabric and analysis of electromagnetic shielding via measurement and empirical equation. *J Mater Process Technol* 2007; 184: 124–130.
7. Shinagawa S, Kumagai Y and Urabe K. Conductive papers containing metallized polyester fibers for electromagnetic interference shielding. *J Porous Mater* 1999; 6: 185–190.
8. Duran D and Kadoglu H. A research on electromagnetic shielding with copper core yarns. *J Textil Apparel* 2012; 22: 354–359.
9. Yidiz Z, Usta I and Gungor A. Electrical properties and electromagnetic shielding effectiveness of polyester yarns with polypyrrole deposition. *Textil Res J* 2012; 82: 2137–2148.
10. Ching IS and Jin TCh. Effect of stainless steel-containing fabrics on electromagnetic shielding effectiveness. *Textil Res J* 2004; 74: 51–56.
11. Knittel D and Schollmeyer E. Electrically high-conductive textiles. *Synth Met* 2009; 159: 1433–1437.
12. Ramachandran T and Vigneswaran C. Design and development of copper core conductive fabrics for smart textiles. *J Ind Textil* 2009; 39: 81–93.
13. Mamunya YeP, Davydenko VV, Pissis P, et al. Electrical and thermal conductivity of polymer filled with metal powders. *Eur Polym J* 2002; 38: 1887–1897.
14. Shateri-Khalilabad M and Yazdanshenas ME. Fabricating electroconductive cotton textiles using graphene. *Carbohydr Polym* 2013; 96: 190–195.
15. Bhat NV, Seshadri DT and Radhakrishnan S. Preparation, characterization and performance of conductive fabrics: cotton + PANi. *Textil Res J* 2004; 74: 155–166.
16. Neruda M and Vojtech L. Verification of surface conductance model of textile materials. *J Appl Res Technol* 2012; 10: 579–585.
17. Zhang Y, Li B, Liu S, et al. Electromagnetic wave absorption properties and mechanical properties of aramid fiber reinforced cement. *Adv Mater Res* 2012; 512–515: 2873–2877.
18. Xue W. Application and molding technique research of aramid fiber composites in radar components. In: *proceedings of 2011 IEEE CIE international conference on radar*, 2011, 2, pp.1402–1405.
19. Hua Y, Yamanaka A and Ni QQ. Electromagnetic shielding properties of super fiber-reinforced composites. *Adv Mater Res* 2010; 123–125: 65–68.
20. Ott HW. *Electromagnetic compatibility engineering*. Hoboken, NJ: John Wiley & Sons, 2009.
21. Wieckowski TW and Jankukiewicz MJ. Methods for evaluating the shielding effectiveness of textiles. *Fibres Textil East Eur* 2006; 14: 18–22.
22. Geetha S, Sathees Kumar KK, Rao Chepuri RK, et al. EMI shielding: methods and materials – a review. *J Appl Polym Sci* 2009; 112: 2073–2086.

23. White D. *A handbook series on electromagnetic interference and compatibility*. Gainesville, VA: Don White Consultants, 1971.
24. Simon R. EMI shielding through conductive plastics. *Polym Plast Technol Eng* 1981; 17: 1–10.
25. Colaneri N and Shacklette L. EMI shielding measurements of conductive polymer blends. *IEEE Trans Instrum Meas* 1992; 41: 291–297.
26. Vojtech L, Neruda M and Hajek J. Planar materials electromagnetic shielding efficiency derivation. *Int J Commun Antenna Propagation* 2011; 1: 1– 10.
27. Keith JM, Janda NB and King JA. Shielding effectiveness density theory for carbon fiber/nylon 6,6 composites. *Polym Compos* 2005; 26: 671–678.
28. Perumalraja R, Dasaradan BS, Anbarasu R, et al. Electromagnetic shielding effectiveness of copper corewoven fabrics. *J Textil Inst* 2009; 100: 512–524.
29. ASTM D 4935-99. Standard test method for measuring the electromagnetic shielding effectiveness of planar materials, June 1999.
30. Horn PS. Some easy *t* statistics. *J Am Statist Assoc* 1983; 78: 930–936.
31. Clingerman ML, King JA, Schulz KH, et al. Evaluation of electrical conductivity models for conductive polymer composites. *J Appl Polym Sci* 2002; 83: 1341–1356.
32. Kim HM, Kim K, Lee CY, et al. Electrical conductivity and electromagnetic interference shielding of multiwalled carbon nanotube composites containing Fe catalyst. *Appl Phys Lett* 2004; 84: 589–591.
33. Yupig D, Shunhua L and Hongtao G. Investigation of electrical conductivity and electromagnetic shielding effectiveness of polyaniline composite. *Sci Technol Adv Mater* 2005; 6: 513–518.
34. Committee for Conformity Assessment on Accreditation and Certification of Functional and Technical Textiles. Specified requirements of electromagnetic shielding textiles, http://www.ftts.org.tw/images/fa003E.pdf (2010, accessed 30 January 2014).